Progress in Oceanography 226 (2024) 103298

Contents lists available at ScienceDirect

Progress in Oceanography

journal homepage: www.elsevier.com/locate/pocean

Physical optima for nitrogen fixation in cyclonic eddies in the Subtropical Northwestern Pacific

Hui Shen [a], Xianhui S. Wan [a,b], Wenbin Zou [a], Mingming Chen [a], Zhendong Hu [a], Senwei Tong [a], Kuanbo Zhou [a], Zong-Pei Jiang [c], Yao Zhang [a], Minhan Dai [a], Shuh-Ji Kao [a,d,*]

[a] State Key Laboratory of Marine Environmental Science & College of Ocean and Earth Sciences, Xiamen University, Xiamen, China
[b] Department of Geosciences, Princeton University, NJ 08544, USA
[c] Ocean College, Zhejiang University, Zhoushan, China
[d] State Key Laboratory of Marine Resource Utilization in South China Sea, Hainan University, Haikou 570228, China

ARTICLE INFO

Keywords:
Upwelling
Light intensity
Nitrogen fixation rates
Diazotrophs
Mesoscale hydrodynamics

ABSTRACT

Nitrogen fixation is a vital new nitrogen source in the oligotrophic ocean. Although our knowledge of the controlling factors of marine nitrogen fixation have increased rapidly, the physical controls, particularly eddies-induced upwelling and light intensity, remain elusive. In this study, conducted in the Subtropical Northwestern Pacific, we measured nitrogen fixation rates (NFR) in two cyclonic eddies (CEs). Our observations in one CE revealed that depth-integrated NFR (INFR) in core stations were significantly higher than in edge stations, indicating that CEs-induced upwelling might enhance nitrogen fixation. However, more intense upwelling in another CE resulted in lower INFR in core stations compared to edge stations. The INFR distributions in CEs were driven by the upwelling intensity, showing a unimodal response, i.e., the maximum INFR appeared at optimal upwelling intensity. This finding reconciles the debate about whether CEs inhibit nitrogen fixation. Additionally, results from light manipulation incubations proved that light intensity is a key driver for the vertically unimodal pattern of NFR, i.e., peaks at the subsurface layer with an optimum light intensity of 20% to 50% of surface PAR. Furthermore, molecular evidence showed that UCYN-A dominated in the upwelling area, while UCYN-B dominated in the non-upwelling area, indicating that CEs-induced physical perturbation regulates the niches of diazotrophs. Taken together, these results suggest that physical dynamics exert profound controls on the spatial heterogeneity of diazotrophic distribution and activity in the Subtropical Northwestern Pacific, providing new insights into the physical drivers of nitrogen fixation on mesoscale hydrodynamics..

1. Introduction

In the vast oligotrophic oceans, biological nitrogen fixation by diazotrophs is a crucial new nitrogen source to the euphotic ecosystem in the nitrogen-depleted surface ocean; this process sustains new production and its subsequent export to the ocean's interior, playing a critical role in marine carbon and nitrogen cycle. (Böttjer et al.,2017; Falkowski, 1997; Karl et al., 1997; Karl et al., 2012; Moore et al., 2013; Sohm et al., 2011). Meanwhile, nitrogen fixation balances the marine nitrogen budget by compensating for nitrogen loss via denitrification and anaerobic ammonia oxidation (Wang et al., 2019; Zehr and Capone, 2020). Since the first report of marine nitrogen fixation in the 1960 s (Dugdale,1961; Dugdale et al., 1964), it has been recognized as a key component of marine biogeochemical studies with the environmental regulation of diazotrophic biogeographic distribution and activity being the central focuses, while physical drivers, such as mesoscale eddies, upwelling, light intensity, etc., remain underexplored and debatable (Ward et al., 2013; Wen et al., 2022; Benavides and Robidart, 2020; Benavides et al., 2021; Church et al., 2009; Kitajima et al. 2009; Lu et al., 2019; Subramaniam et al. 2013; Liu et al., 2023b). Via investigation of the impact of physical divers on nitrogen fixation, this study tried to address this knowledge gap.

Mesoscale eddies are ubiquitous hydrodynamic processes in the global ocean, exerting profound controls on nutrient redistribution and subsequent biogeochemical dynamics (McGillicuddy, 2016). Cyclonic eddies (CEs) cause sub-surface water to lift due to the divergence of the surface water, while anticyclonic eddies (AEs) cause the convergence of surface water to deepen the isopycnal layer. CEs enhance the

* Corresponding author at: State Key Laboratory of Marine Environmental Science & College of Ocean and Earth Sciences, Xiamen University, Xiamen, China.
E-mail address: sjkao@xmu.edu.cn (S.-J. Kao).

https://doi.org/10.1016/j.pocean.2024.103298
Received 29 April 2023; Received in revised form 30 May 2024; Accepted 19 June 2024
Available online 30 June 2024

entrainment of subsurface nutrients into the eutrophic zone, stimulating phytoplankton growth and primary production (Falkowski et al., 1991; Oschlies and Garçon, 1998; Liu et al., 2024). Meanwhile, the uplifted isopycnal layer in CEs carries the plankton from the deeper layer to the surface ocean, alleviating the light limitation for photoautotrophs. This dual supply of nutrients and solar energy turns the euphotic zone in CEs into a productivity hotspot (Gruber et al., 2011; McGillicuddy, 2016).

To date, only a few studies have explored the impact of mesoscale eddies on nitrogen fixation in the oligotrophic oceans (Benavides et al., 2021; Wilson et al. 2017; Church et al., 2009; Davis and McGillicuddy, 2006; Dugenne et al., 2023; Fong et al., 2008; Holl et al., 2007; Liu et al., 2020). From a traditional perspective, nitrogen fixation is expected to be suppressed in the CEs where subsurface water with low temperature and high nutrient upwells, as diazotrophs might be beaten by the non-diazotrophic phytoplankton in this low temperature and high nitrate conditions (Dekaezemacker and Bonnet, 2011; Holl and Montoya, 2005; Holl et al., 2007; Luo et al., 2012). On the contrary, AEs may favor the diazotrophs as a result of higher abundance of diazotrophs and nitrogen fixation rate (NFR) have been observed in AEs compared to those in CEs in different regions of the global ocean (Benavides et al., 2021; Wilson et al. 2017; Church et al., 2009; Davis and McGillicuddy, 2006; Dugenne et al., 2023; Fong et al., 2008; Holl et al., 2007; Liu et al., 2020), supporting the hypothesis that CEs are unfavorable for diazotrophs. This paradigm, however, is complicated by several lines of evidence 1), the unicellular cyanobacterial diazotroph group A (UCYN-A) is recently found ubiquitously and remains active in the high-nutrients and low-temperature environments (Harding et al. 2018; Mills et al., 2020; Tang et al. 2019; Shiozaki et al., 2020), indicating nitrogen fixation maybe not necessarily inhibited in the CEs when UCYN-A is the dominant diazotroph; 2) the upwelling water with excess phosphate (i.e., the water mass with initial N:P < 16) and the subsequent Redfieldian consumption of nitrogen and phosphate by the phytoplankton leads to elevated P* (an indicator of excess P), which in turn fuels the growth of diazotrophs (Deutsch et al., 2007; Karl & Letelier, 2008; Subramaniam et al., 2013; Ward et al., 2013). Moreover, most previous studies only have limited spatial and temporal resolution on sampling stations (i.e., at only one station in one eddy or one stage of the eddy life) (Dugenne et al., 2023; Holl et al., 2007; Liu et al., 2020), leading to a fragmented understanding of nitrogen fixation in response to the CEs. To accurately evaluate the impact of CEs on nitrogen fixation at different stages, higher spatial and temporal resolution studies are needed.

In addition to temperature and nutrients, light intensity also plays an important role in regulating the growth and activity of photoautotrophic diazotrophs. In the well-stratified tropical and subtropical oceans, the measured NFR often showed a subsurface maximum. The max NFR was located at around 30 m where in-situ light intensity was lower than that at the surface (Lu et al., 2019; Shiozaki et al., 2017; Wen et al., 2022). Given that the other physical–chemical properties (such as temperature, salinity, nutrients, etc.) are mostly homogenous in the upper mixed layer in the oligotrophic ocean, we hypothesized that the subsurface peaks of NFR in the field are driven by light intensity and the NFR-irradiance curve in the field might not follow these photosynthetic models conducted in the laboratory for different photoautotrophic diazotrophs (Kara et al., 2000; Breitbarth et al., 2008; Foster et al., 2010; Garcia et al., 2013; Gradoville et al. 2021; Lu et al., 2018; Pyle et al., 2020; Villareal, 1990; Webb et al., 1974). Nevertheless, the impact of light intensity due to the shoaling of the isopycnal layer on nitrogen fixation in the CEs has not yet been systematically examined.

The Subtropical Northwestern Pacific is a hot spot for marine nitrogen fixation owing to its high temperature and low surface nitrate concentration, which favor the growth of diazotrophs when phosphate and iron are available (Karl et al., 2012; Wang et al., 2019; Ward et al., 2013; Wen et al., 2022). Meanwhile, this region is also home to the most complex oceanic circulation systems, with the westward flowing North Equatorial Current (NEC), carrying subducted North Pacific Tropic Water (NPTW), which splits into the equatorward flowing Mindanao Current and the northward flowing Kuroshio upon reaching the Philippine coast (Fig. 1a-b) (Qiu & Lukas,1996; Toole et al., 1990). Mesoscale eddies are also very active in this region due to the baroclinic instability associated with vertical velocity shears between the surface Subtropical Countercurrent and the underlying NEC, stimulating biogeochemical processes here, such as primary production, nitrification, etc. (McGillicuddy, 2016; Qiu, 1999; Yang et al., 2013; Liu et al., 2023a; Liu et al., 2024). Additionally, previous studies have shown that photoautotrophic cyanobacterial diazotrophs (UCYN-A, UCYN-B, or *Trichodesmium*) were dominant in this region (Chen et al., 2019; Wen et al., 2022). Therefore, the Subtropical Northwestern Pacific is an ideal area to test the impact of physical drivers (mesoscale eddies-induced upwelling and light intensity) on nitrogen fixation.

In this study, we examined the response of nitrogen fixation to different gradients of physical drivers by utilizing the $^{15}N_2$ labelling method, molecular biology techniques and the incubation device providing artificial sunlight with programmed time intervals. Our results suggest that physical drivers play a critical role in structuring the distribution of diazotrophic activity.

2. Sampling and methods

2.1. Cruise and stations

Two research cruises were conducted in the Subtropical Northwestern Pacific to investigate the impact of CEs on nitrogen fixation and to examine the regulation of light intensity on NFR. The first cruise (*KK1902 'SILICON EDDY'*) took place onboard R/V *Tan Kah Kee* between March 15 and April 20, 2019. The second cruise (*KK2007*) was conducted between December 23, 2020 and February 07, 2021, onboard R/V *Tan Kah Kee*.

The hydrographic data were collected using the SeaBird SBE 911plus CTD, which recorded temperature, salinity, fluorescence, and photosynthetically active radiation (PAR). During the *KK1902* cruise, near-real-time high temporal resolution (1 day) of satellite-based sea level anomaly (SLA) values and geostrophic current vectors were used to identify CEs before sampling. Two CEs (CE4 and CE2) were targeted for our sampling (Fig. 1 a-b). The vessel followed the trajectory of CEs to explore the temporal and spatial evolution by using the Lagrangian method. Four transects spanning different areas (core, edge) were selected for collecting hydrological data (transect 1 in CE4; transects 2, 3, 4 in CE2) (Fig. 1 c-g; Table S1). Notably, three times repeated observations were conducted in CE2. In addition, eleven stations in these four transects were selected for NFR incubations, which were divided into core and edge stations by the differences in hydrographic characteristics among stations (Fig. 2; Table S1). The station classification was proven reasonable by principal component analysis (Fig. S1). In this region full of AEs and CEs, we can hardly define a reference station for comparison. In addition, light manipulation incubations were carried out at one selected station during the *KK2007* cruise to examine the regulation of light intensity on NFR (Fig. 1a-b).

2.2. Sampling and on-board incubations

During the cruise *KK1902*, water samples were collected for incubations using 12 L Niskin bottles that were attached to the CTD rosette and sub-sampled into 1.2 L polycarbonate bottles that had been pre-rinsed by 1 N HCl. The polycarbonate bottles were rinsed with Milli-Q and sample water before filling them up. The six to seven layers were selected at each station in the upper 180 m to conduct NFR incubations (Fig. 2). NFR were determined using the enriched water method (Mohr et al., 2010; Wilson et al., 2012; Lu et al., 2018, 2019). Briefly, to prepare $^{15}N_2$ enriched seawater, 2 L of surface seawater were filtered through a 0.22 μm filter (Millipore) and transferred into 2 L Tedlar bags without headspace. Then, 20 ml of $^{15}N_2$ (isotopic enrichment 98.9 %, chemical purity $>$ 99.9 %, Cambridge Isotope Laboratories, Inc.) was

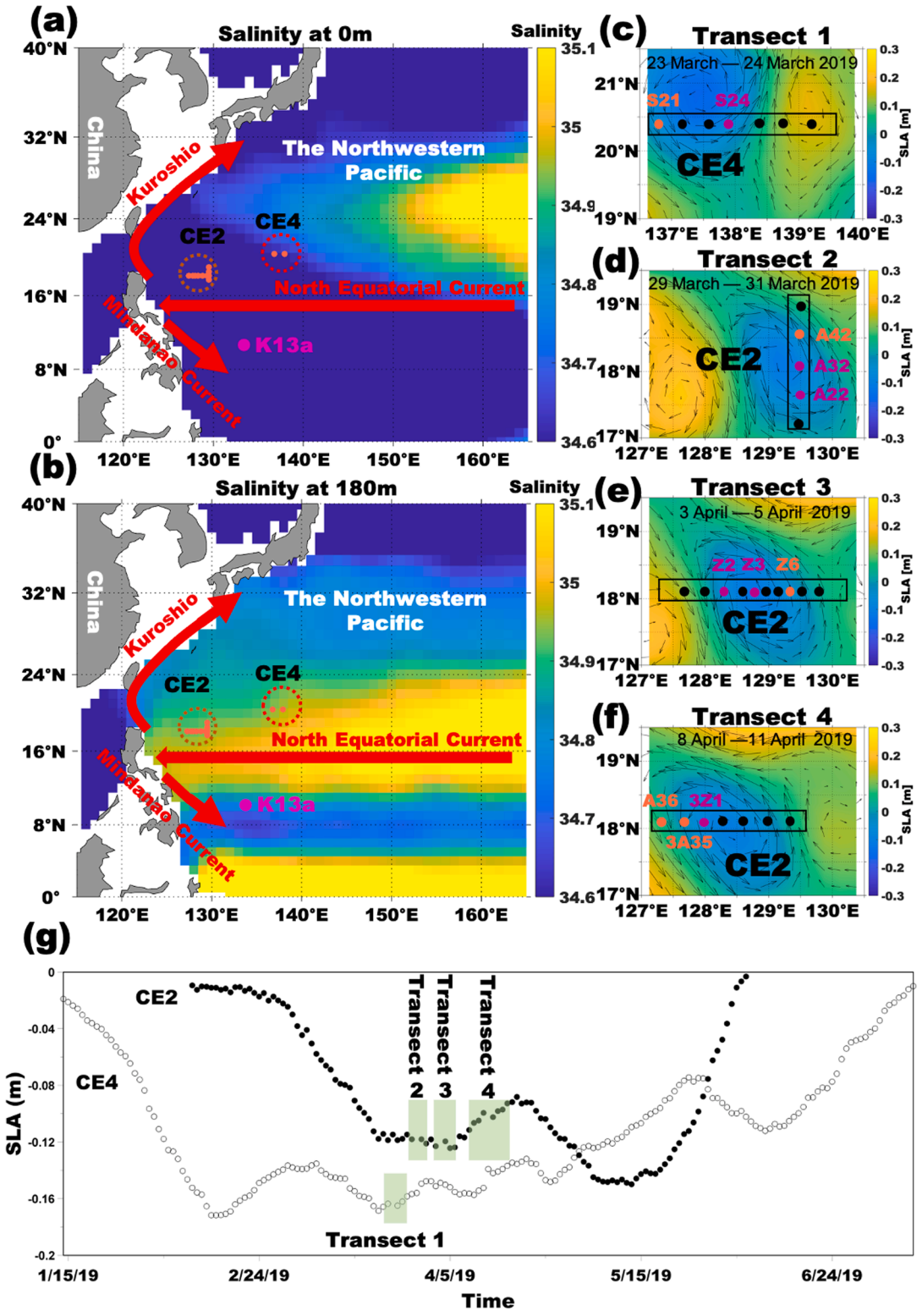

Fig. 1. Overview of the oceanic circulation systems of the study area and sampling information during the study. The distribution of annual average salinity for 2019 at the sea surface (a) and at 180 m (b) in the study region. The two circles denote the location of CE4 and CE2 in the Subtropical Northwestern Pacific and the orange dots in the circles are stations for NFR incubations in *KK1902*. Red arrows present the North Equatorial Current, Mindanao Current and the Kuroshio. The salinity data are downloaded at http://data.argo.org.cn. The pink dot presents the K13a station for light manipulation incubations in *KK2007*. Four transects in two CEs are in Fig. 1 c-f. The sampling time period for four transects are indicated at the top of each figure. Black dots are stations for only collecting hydrological data. Purple dots (core stations) and orange dots (edge stations) are stations for both collecting hydrological data and conducting NFR incubations. The background is reprocessed daily SLA values at the midpoint of the time period for each transect. The black arrows are geostrophic current vectors. SLA values and data for geostrophic current vectors are downloaded at https://marine.copernicus.eu/https://marine.copernicus.eu/. (g) The lifespan-evolution SLA values in the center of CE2 and CE4 (time resolution: 1 day). Filled dots represent CE2 and hollow dots represent CE4. Green shadows show the sampling period for four transects in this study. (For interpretation of the references to color in this figure legend, the reader is referred to the web version of this article.)

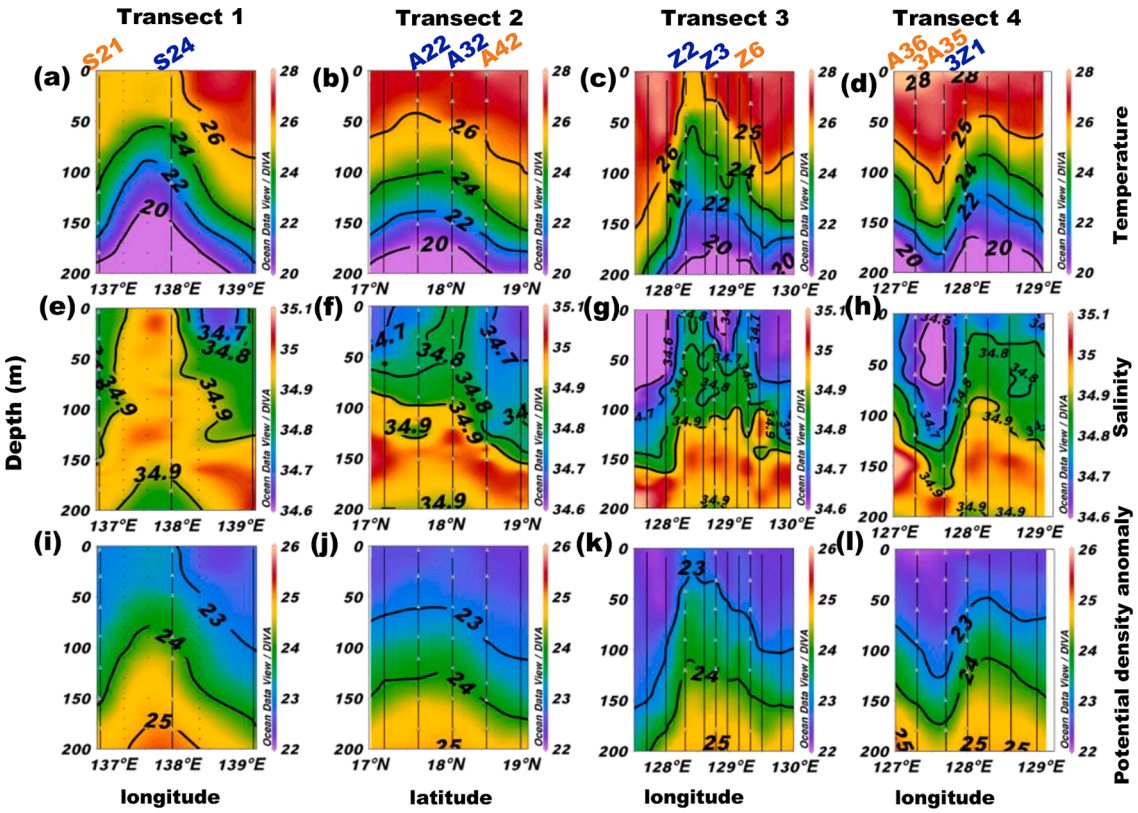

Fig. 2. Vertical profiles of temperature, salinity and potential density anomaly in the four transects. (a-d): Temperature (℃); (e-h): Salinity; (i-l): Potential density anomaly (kg m^{-3}). Gray triangles represent layers for NFR incubations. The colors of the name of core stations and edge stations are blue and orange, respectively. (For interpretation of the references to color in this figure legend, the reader is referred to the web version of this article.)

injected into each Tedlar bag. The Tedlar bag was slapped to dissolve the $^{15}N_2$ gas until all visible bubbles dissolved. The $^{15}N_2$ enriched water was used within 12 h to prevent leakage of $^{15}N_2$ in the Tedlar bag. Then, 100 ml $^{15}N_2$ enriched water was slowly injected into each 1.25 L polycarbonate bottle. Any headspace after tracer injection in the incubation bottles was amended with in-situ seawater. The final $^{15}N_2$ enrichment in incubation bottles were not measured directly during this cruise. However, the $^{15}N_2$ atom % were measured in the shore lab by mimicking the onboard incubation procedures and conditions using a membrane inlet mass spectrometry (MIMS) (Text S1). The $^{15}N_2$ atom % in the simulated incubations ranged from 8.30 to 8.55 atom % (Table S2), with a mean ± SD of 8.42 ± 0.09 atom % (n = 6). The average value of 8.42 atom % was used for calculating the NFR in the *KK1902*. The water samples were incubated on deck and all incubation bottles were cooled by flowing surface seawater. Light conditions of the incubators were manipulated using neutral density and blue filters (061 Mist blue; 172 Lagoon blue) to achieve near in-situ light intensity (Lu et al., 2018). The actual on-deck light intensity during the incubations was monitored using a flat 2π PAR sensor (PQS 1 PAR Quantum sensor) at one-minute intervals. The incubators were covered with an opaque film at night to prevent any light contamination from the vessel. The samples were incubated for 24 h with triplicates. Particulate nitrogen (PN) samples were collected by using pre-combusted (450 ℃, 4 h) 25 mm glass fiber filters (GF/75, 0.3 μm; Advantec) with a pressure < 200 mm Hg at the beginning (T0) and end (T1) of the incubations. All filters were stored at − 20 °C on board immediately after filtration.

During the cruise *KK2007*, water samples from four depths (5 m, 25 m, 50 m, 120 m) in K13a were collected for the light manipulation incubations (Fig. 1a-b). Differently, the modified bubble release method was used during this cruise due to the less perturbation induced by the modified bubble release method (Chang et al., 2019; White et al.,2020). The $^{15}N_2$ atom % in the incubation bottles was directly measured by MIMS here. In addition, to quantify and compare the optimal light intensity for the diazotrophs at different depths, the light manipulation incubations were performed utilizing an artificial simulated periodical sunlight system (Hydra® 64HD, AquaIllumination) and temperature-controlled incubators. Six gradients of light intensities (corresponding in-situ depth at 2 m, 5 m, 25 m, 50 m, 120 m, and depth of 0.1 % surface PAR (sPAR)) were set for incubation at each depth. Temperatures in the incubators were set according to in-situ temperature. Incubations lasted for 24 h (12 h periodical sunlight and 12 h dark). Triplicated PN samples were collected at the beginning (T0) and end (T1) in the incubations using the procedure described above.

2.3. PN concentration and δ^{15}N-PN measurement

All filters were freeze-dried for 48 h before measurement. PN was oxidized to nitrate using the wet digestion method with slight modification (Knapp et al., 2005; Wan et al., 2018; Xu et al., 2019). In brief, each filter was placed into a 12 ml pre-combusted (450 ℃, 4 h) borosilicate glass tube with 0.3 ml purified persulfate oxidizing reagent and 5 ml Milli-Q water. The persulfate (ACS-grade, Merck, German) was recrystallized at least three times then adding NaOH (ACS-grade, Merck, German) and Milli-Q water as a ratio: 6 g persulfate and 6 g NaOH and 100 ml Milli-Q water. The residual nitrate in the reagent was measured to ensure nitrate concentration was less than 2 μmol L^{-1} (reagent blank). The caps were closed tightly once regent and Milli-Q water were added. Then the tubes were autoclaved at 120 °C for one hour. Nitrate concentration after oxidation (containing the particulate sample, reagent blank, and filter blank) was measured by the chemiluminescence method (Braman and Hendrix, 1989). The blank of filters was less than 6 nmol N after the cruise. Regent blank and filter blank account for less than 1 % and 3 % of the total N content in tubes, respectively (Table S3). Isotopic values were measured by the denitrification bacterial method

coupled Gasbench-Isotopic Ratio Mass Spectrometer (Thermo Fisher Delta V) (Sigman et al., 2001; Casciotti et al., 2002). International isotopic standards of NO_3^-: USG34, IAEA3, and USGS32, were used to calibrate the $\delta^{15}N\text{-}NO_3^-$. Accuracy (pooled standard deviation) was better than ± 0.3 ‰ according to analyses of these standards at a level of 20 nmol N. We also conducted tests to validate our method for NFR determination (Text S2; Fig. S2).

2.4. Rate calculation

The nitrogen fixation rates were calculated according to (Montoya et al., 1996).

$$NFR = \frac{1}{\Delta T} \times \frac{APN_f - APN_0}{AN_2 - APN_0} \times \frac{PN_f + PN_0}{2} \quad (1)$$

NFR is the nitrogen fixation rate in nmol N L^{-1} d^{-1}; ΔT is incubation length; APN_0 and APN_f are the initial and final ratio of ^{15}N% of the PN samples (calculated from the measured isotopic value); AN_2 is $^{15}N_2$ enrichment in the incubation bottles; PN_0 and PN_f is the initial and final concentration of particulate nitrogen.

We also calculated the limit of detection (LOD) according to the propagation of uncertainty in each measured experimental parameter with following White et al. (2020). LOD ranges from 0.02 to 0.74 nmol N L^{-1} d^{-1} in this study (Table. S4). All of our NFR were over LOD except A32_130 m, A32_150 m, A42_150 m and Z3_120 m.

The trapezoidal integration method was used to integrate nitrogen fixation rates (INFR) of the water column.

2.5. nifH gene copies measurements

Copies of *nifH* gene were collected and quantified in only four stations in CE2 (Z2, Z6, A36, and 3Z1). In brief, 2 L of seawater were filtered through 0.22 μm pore size polycarbonate filters (Supor-200, Pall Gelman) for DNA extraction. All filters were flash-frozen in liquid nitrogen and then transferred to − 80℃ on board until further analysis. DNA was extracted using the phenol–chloroform-isoamyl alcohol method with minor modifications (Massana et al., 1997; Chen et al., 2019). The concentration and purity of the genomic DNA were detected using a NanoDrop spectrophotometer (Thermo Scientific 2000/2000c). In this study, nine major diazotrophic groups (UCYN-A1, UCYN-A2, UCYN-B, UCYN-C, *Trichodesmium*, Het1, Het2, Het3, γ-24774A11) were quantified via TaqMan qPCR assays. Specific primer and probe sets followed previous studies (Table S5) (Church et al., 2005; Thompson et al., 2014; Foster et al., 2007; Moisander et al., 2008).The thermocycling conditions and reaction mixtures for qPCR followed by Chen et al. (2019). Triplicate qPCRs were run for each environmental DNA sample and each standard on a CFX96 Real-Time System (Bio-Rad Laboratories). Negative controls without templates were also included to test for contamination. A standard curve was made using serial dilutions of quantified, linearized plasmid containing target sequence for each run. The amplification efficiencies of PCR were always between 95 % and 100 %, with R^2 values of standard curves > 0.99 (Table S5). The quantification limit of the qPCR reactions was one *nifH* gene copy per reaction according to the estimates from maximum Ct-values generated by quantifiable samples (at least two of the three replicates were amplified).

2.6. Statistical analysis

The significance of differences in NFRs and environmental parameters between different stations were tested by *t* test and analysis of variance (ANOVA) followed by the Tukey test, respectively, using SPSS. A significance level of $p < 0.05$ was applied. Generalized additive models (GAM) was used to fit the correlation between NFR and environmental parameters by R (Version: '2023.12.1 + 402'; package: 'mgcv').

3. Results

3.1. Hydrological distribution

During the *KK1902* cruise, two CEs (CE2 and CE4) were captured by the SLA values and geostrophic current vectors (Fig. 1 c-f). The shape of those two CEs was approximate circular with diameters of 150 – 300 km. Those two CEs generally went through formation − mature − decay in their lifespan and gradually moved westward (Fig. 1 c-g). During the observational period, the SLA values in the eddy center in the CE4 were − 0.17 to − 0.15 m (mature state) and that in the CE2 were − 0.07 to − 0.12 m (mature state) (Fig. 1 g), indicating CE4 might have more intense upwelling than CE2.

The vertical profiles of temperature, salinity, and potential density in the CEs showed similar dome-shape structures (Fig. 2). Isothermals, isohalines, and isopycnals were uplifted at the range of 50 m to 150 m in core stations compared to edge stations in the CEs. CE4 exhibited more pronounced shoaling of the subsurface water compared to CE2 (Fig. 2 a, e, i), demonstrating a more intense upwelling during the sampling period. This observation aligns with the differences in SLA values at the eddy centers between CE4 and CE2 (Fig. 1g). Sea surface temperature (SST) progressively decreased from the edge stations to the core stations in each transect (Table 1 and Fig. 2 a-d). The 180 m-average temperatures in core stations were significantly lower than those in edge stations ($p = 0.003$; Table S6, Table 1). In all transects, the high salinity water, the NPTW, was uplifted from about 150 m depth to 0–100 m depth (Fig. 2 e-h; Fig. S3). Especially, in the core of CE4, the mainstream of NPTW outcropped to the surface and pushed the originally superincumbent water to the side, showing a more intense upwelling in CE4 than CE2. Consequently, the core stations had higher sea surface salinity (SSS) than the edge stations (Table 1). In core stations, the 180 m-average salinity were also significantly higher than in edge stations ($p = 0.013$; Table S6, Table 1). The potential density showed a similar spatial pattern with temperature (Fig. 2 i-l). These results suggested the hydrological structure was reorganized by the CEs-induced upwelling.

Deep chlorophyll maximum (DCM) layers were significantly shallower accompanied with higher fluorescence value in DCM in the core stations compared to that in edge stations (Fig. 3 a-d, $p = 0.01$ for DCM; $p = 0.169$ for fluorescence in DCM, Table S6). However, there is no significant difference in the depth of 0.1 % sPAR between core and edge stations ($p = 0.207$, Fig. 3 a-d, Table S6). PN concentration was around 0.3 μmol L^{-1} with slight variation between core and edge stations in the upper euphotic zone (Fig. 3 e-h). In the deeper euphotic zone, PN concentration decreased to 0.1–0.2 μmol L^{-1}, with the lowest concentration observed in the cores of CEs in each transect (Fig. 3 e-h), indicating upwelling deep water with relatively lower PN concentration diluted or replaced the originally superincumbent water which have had relatively higher PN concentrations. This dilution effect may influence the subsequent biogeochemical processes. However, the 180 m-integrated PN concentrations in core stations were not significantly different from that in the edge stations ($p = 0.369$, Table S6), showing plankton potentially prospered in the upper euphotic zone in the core of CEs even dilution effect was dominated here.

3.2. Nitrogen fixation rates and diazotrophs distribution

The surface NFR (sNFR) varied between 0.6 to 2.5 nmol N L^{-1} d^{-1} in all stations (Table 1). The sNFR in the core station demonstrated significantly higher than that in the edge stations in CE2 ($p = 0.002$, Table S6). The maximum NFR in the vertical profile (ranging from 1.1 to 4.6 nmol N L^{-1} d^{-1}; Table S4) were observed at around 30 m except for the A32 station. Below the depth of maximum NFR, the NFR decreased steeply (Fig. 3i-l; Table S4). Therefore, the profiles of NFR at nearly all investigated stations (10 out of 11) exhibited a vertically unimodal pattern (Fig. 3 i-l).

The INFR ranged from 99 to 275 μmol N m^{-2} d^{-1} and showed clear

Table 1
Environmental parameters and nitrogen fixation rates. Average T and S are calculated with corresponding data within 180 m. Fluorescence is fluorescence values in DCM. IPN and INFR are depth-integrated PN and NFR within 180 m. E denotes light attenuation coefficient. ND means no data.

Stations	SST (°C)	Average T (°C)	SSS	Average S	DCM (m)	Fluorescence (mg m^{-3})	Depth of 0.1 %PAR (m)	E (m^{-1})	IPN (mmol m^{-2})	sNFR (nmol N L^{-1} d^{-1})	INFR (μmol N m^{-2} d^{-1})
S21	25.5	24.2	34.84	34.86	155	0.503	162	0.043	60.32	0.8	207
S24	25.5	22.5	34.95	34.94	105	0.463	ND	ND	51.11	1.1	165
A22	26.8	23.9	34.76	34.86	114	0.549	130	0.053	48.07	1.7	168
A32	26.6	23.9	34.82	34.89	127	0.658	ND	ND	49.55	2.4	136
A42	27.5	25.0	34.74	34.82	136	0.546	157	0.044	50.39	1.5	138
Z2	25.9	22.8	34.77	34.89	87	0.585	159	0.043	44.24	2.5	239
Z3	26.7	23.4	34.75	34.86	100	0.459	162	0.043	37.82	2.3	275
Z6	27.2	24.6	34.73	34.85	136	0.474	159	0.041	45.78	0.7	194
3A35	27.7	25.7	34.60	34.71	152	0.444	179	0.039	46.23	0.6	99
a36	28.1	25.4	34.65	34.78	112	0.488	159	0.043	39.75	1.1	132
3z1	27.6	24.0	34.77	34.88	115	0.567	159	0.043	36.74	2.0	202

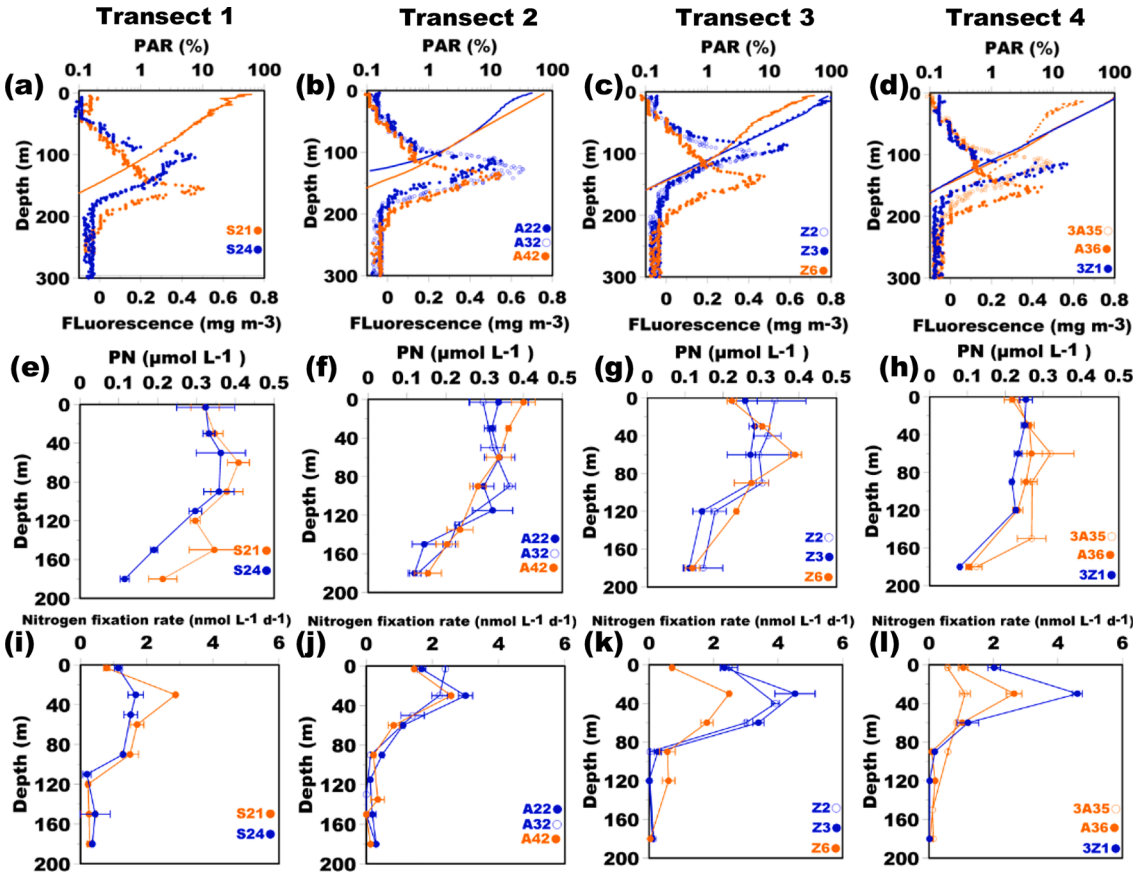

Fig. 3. Depth profiles of PAR, Fluorescence, PN and NFR in the four transects. (a-d): Depth profiles of PAR and fluorescence; (e-h): PN concentrations; The error bars depict one standard deviation of triplicate samples. (i-l): nitrogen fixation rates in four transects. The error bars depict one standard deviation of triplicate rate measurements. In some cases, the error bars are smaller than the symbols. The blue color shows results in core stations and the orange color denotes results in edge stations. (For interpretation of the references to color in this figure legend, the reader is referred to the web version of this article.)

spatial gradients (Table 1). In the CE2, INFR in core stations were significantly higher than that in edge stations ($p = 0.046$, Table S6). Furthermore, both INFR and sNFR exhibited a significant negative correlation with SLA ($R^2 = 0.52$, $p < 0.05$; $R^2 = 0.51$, $p < 0.01$, respectively; Fig. 4 a, c) and a positive correlation with salinity in the CE2 ($R^2 = 0.41$, $p = 0.06$; $R^2 = 0.67$, $p < 0.01$, respectively; Fig. 4 b, d), implying nitrogen fixation were stimulated in the core of the CE2. However, in the CE4, showing more intense upwelling than CE2, the core station had lower INFR than the edge station (core: 165 ± 33 μmol N m^{-2} d^{-1} edge: 207 ± 25 μmol N m^{-2} d^{-1}, Table 1). These findings suggested different responses of nitrogen fixation to the CEs-induced upwelling, indicating complex impacts of the mesoscale-eddies-associated physical processes on nitrogen fixation.

UCYN-B and UCYN-A (UCYN-A1 plus UCYN-A2) were the dominant species, accounting for approximately 95 % of total *nifH* gene copies (Fig. S4). The γ-24774A11 gene was consistently detected with one to two orders of magnitude lower than that of UCYN-A and UCYN-B. UCYN-C and *Trichodesmium* were detectable but contributed a minor fraction of the total diazotrophs (Fig. S4). Het1, Het2, and Het3 were all not detectable in the most of samples (Fig. 5). The vertical distribution of diazotrophs in four stations in CE2 showed a similar pattern (Fig. 5). In the upper 90 m, the *nifH* gene copies of UCYN-A were more abundant than those of UCYN-B in the Z2, Z6, and 3Z1, while a reversed relationship was observed in the A36 (Fig. S4). In the deeper euphotic zone,

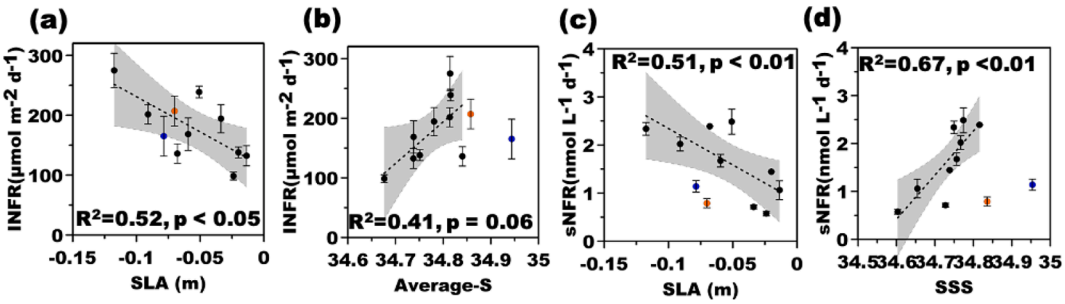

Fig. 4. Correlation between INFR, sNFR, SLA and salinity. INFR against SLA values (a) and average salinity within 180 m (b); sNFR against SLA values (c) and SSS (d). Blue dots (S24, core station) and orange dots (S21, edge station) are data in CE4. Linear regressions are conducted using data in CE2. Dashed lines denote the best regression and grey shadows represent 95 % confidence intervals. Error bars represent the standard deviation from triplicate samples. (For interpretation of the references to color in this figure legend, the reader is referred to the web version of this article.)

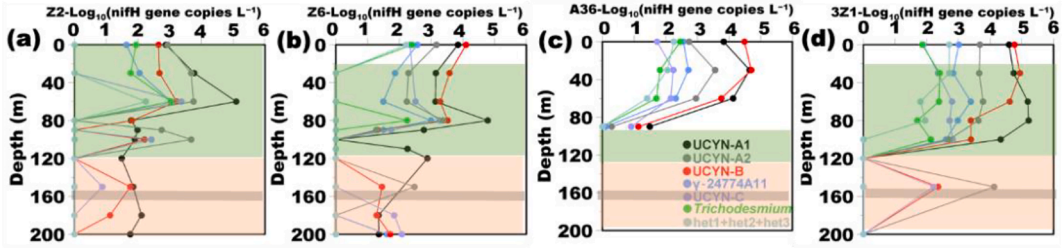

Fig. 5. Depth profiles *nifH* gene copies in four stations in Z2 (a), Z6 (b), A36 (c), and 3Z1 (d) in CE2. Green shadow means the area with a salinity of 34.8 ± 0.1, and orange shadow means the area with a salinity over 34.9. The gray bars denote a depth of 0.1 % sPAR. (For interpretation of the references to color in this figure legend, the reader is referred to the web version of this article.)

nifH gene copies of UCYN-A were always more abundant than that of UCYN-B (Fig. 5). Diazotrophs were also detectable below the euphotic zone (Fig. 5).

3.3. Results of light intensity manipulation incubations

During the light manipulation incubations, the NFR showed a unimodal response to the light intensity at all investigated depths (Fig. 6). Specifically, NFR increased with light intensity up to an optimal level, and NFR declined with further increases in light intensity. The optimal light intensity was approximately 725 μE m^{-2} s^{-1} (daily average light intensity, the same hereinafter; 50 % of sPAR, corresponding to the in-situ light intensity at 5 m) for the samples collected from 5-50 m. For the sample collected from 120 m, the optimal intensity was around 290 μE m^{-2} s^{-1} (20 % of sPAR, corresponding to the in-situ light intensity at 25 m). These results suggest that diazotrophs in the upper euphotic zone have a high light demand, whereas those near the base of the euphotic zone have acclimated to low-light conditions and maybe vulnerable to increased light intensity.

4. Discussion

4.1. CEs-induced upwelling exerts a unimodal control on nitrogen fixation in the Subtropical Northwestern Pacific

Previous studies have demonstrated the profound influence of eddy dynamics on marine biogeochemistry, including nutrient distribution (Gruber et al., 2011; McGillicuddy, 2016; Liu et al., 2023a; Rohr et al.,2020), primary production (Falkowski et al., 1991; Oschlies and Garçon, 1998; Liu et al.,2024), export production (Liu et al.,2024; Guo et al.,2024) and phytoplankton community structure (Liu et al., 2020).

However, only a few efforts have been devoted to exploring the underlying mechanism of response of nitrogen fixation to eddies (Benavides et al., 2021; Wilson et al. 2017; Church et al., 2009; Davis and McGillicuddy, 2006; Dugenne et al., 2023; Fong et al., 2008; Holl et al., 2007; Liu et al., 2020). These studies generally conclude that upwelling has a negative impact on nitrogen fixation in the CEs due to the introduction of low-temperature and nitrate-enriched waters, as well as the dilution effect on diazotrophs in surface waters. (Dekaezemacker and Bonnet, 2011; Dugenne et al., 2023; Holl et al., 2007; Luo et al.,

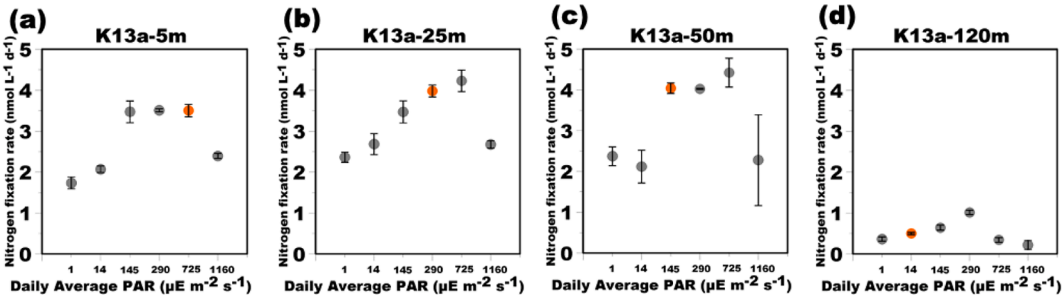

Fig. 6. Results of light manipulation incubations in K13a in *KK2007*. Orange dots denote NFR at in-situ light intensity. Error bars represent the standard deviation from triplicate samples. In some cases, the error bars are smaller than the symbols. (For interpretation of the references to color in this figure legend, the reader is referred to the web version of this article.)

2012). Our observations in CE4 were in line with this view showing INFR in core station was lower than that in edge station (Table 1). Unexpectedly, our investigations in the CE2 showed the higher INFR in the core stations (Fig. 4), indicating that some other favorable factors induced by upwelling in CE2 can compensate for those negative impacts on nitrogen fixation.

Interestingly, high NFR (i.e., > 2.5 nmol N L^{-1} d^{-1}) were detected when water with a specific salinity of 34.8 ± 0.1 was uplifted to a depth of around 30 m (Fig. S5, Fig. 7 a, b). Nevertheless, the NFR measured in the water with a salinity of 34.8 ± 0.1 were consistently low when the water mass was not uplifted, suggesting that diazotrophic activity was enhanced when the water was upwelled into the upper euphotic zone (Fig. S5). Additionally, in the core station of CE4 (S24), the mainstream of NPTW outcropped to the surface, and the water mass with a salinity of 34.8 ± 0.1 incidentally upwelled at the edge station (S21) (Fig. 2 e). Higher INFR in edge stations than that in core stations (Table 1), reinforced the stimulation of NFR when the water with a salinity of 34.8 ± 0.1 was uplifted to the upper euphotic zone by the CEs. The water mass with a specific salinity of 34.8 ± 0.1 have the potential to enhance nitrogen fixation which need further investigation.

In this study, UCYN-A and UCYN-B were the dominant diazotrophs, which were detectable throughout the upper 200 m despite a rapid decrease in the deeper euphotic zone (Fig. 5). In the non-uplifted NPTW, UCYN-A and UCYN-B might be exported from the upper layer by embedding in large particulate matter or forming aggregates (Bonnet et al., 2023a; Farnelid et al., 2019). Meanwhile, the N:P ratio in the deeper Pacific Ocean was found to be below the Redfield Ratio (16:1) owing to denitrification in the East Tropic Pacific, indicating an excess of phosphorus compared to nitrogen (Deutsch et al., 2007; Gruber and Sarmiento, 1997). The upwelling of subsurface water with N:P < 16 would lead to an excess of phosphorus following the Redfieldian uptake of N and P by phytoplankton, which in turn fuels the growth of diazotrophs (Deutsch et al., 2007; Karl and Letelier, 2008; Subramaniam et al., 2013; Ward et al., 2013). Additionally, CEs-induced upwelling can also increase the supply of iron, contributing to the enhancement of nitrogen fixation in the CEs (Boyd and Ellwood, 2010; Bonnet et al., 2023a,b). Sub-mesoscale fronts can drive the vertical nutrient supply and stimulate the phytoplanktonic growth (Guo et al., 2022; Guo et al., 2024). However, current sampling scheme does not allow us to discuss how sub-mesoscale processes affect nitrogen fixation.

Combining this, water mass with a salinity of 34.8 ± 0.1, mixed NPTW and surface water, containing the diazotrophic seeds and adequate nutrients, had the potential for enhancing nitrogen fixation in the process of upwelling. Diazotrophic seeds may be limited by low light and low temperature in the deeper water of origin, waiting to alleviate these limitations by upwelling (Gradoville et al., 2021; Fu et al., 2014).

The dilution effect on PN was observed in the deeper euphotic zone, particularly in CE4 (Fig. 3 e-h). however, PN concentration in the upper euphotic zone and fluorescence at the DCM were comparable in the core stations of CE4 and CE2 (Fig. 3 a-h), indicating non-diazotrophic phytoplanktonic seeds in the deep NPTW also flourished during the upwelling. Recently, Liu et al., (2024) reported that *meso*-zooplanktons were two-fold increased within the core of CE2, suggesting that overall grazing pressure was enhanced even primary production was also increased. The balance between phytoplanktonic growth and grazer's predation may regulate the PN concentration in the upper euphotic zone in the CEs. Diazotrophs maybe concomitantly subject to grazing pressure which exert a negative effect for the flourishing diazotrophs during the upwelling (Wang and Luo, 2022).

However, diazotrophs in NPTW (salinity over 34.9) might undergo low-light and low-temperature acclimation, leading to less activity to light and temperature enhancement during this intense upwelling in CE4 (Yi et al.,2020) (Fig. 6). Although we have not obtained diazotrophic information in CE4, we speculated that diazotrophic abundance in the upper euphotic zone in the core of CE4 was relatively low due to the flushing of high-salinity water with low diazotrophic activity. Therefore, excessive intensity of upwelling prevented diazotrophs from growth which might result in reduced nitrogen fixation rates. Our results in two CEs revealed that nitrogen fixation showed a unimodal response to the intensity of CEs-induced upwelling in the Subtropical Northwestern Pacific.

4.2. *Light intensity exerts a key control on the vertically unimodal pattern of nitrogen fixation rates*

Light intensity is a crucial regulator of biogeochemistry in the euphotic zone, which is the primary source of energy and organic matter for oceanic plankton (Falkowski and Raven, 2013). Our light manipulation incubations performed at the K13a demonstrated a unimodal response of NFR to varied light intensity across all the investigated depths. The optimal light intensity was ~ 725 μE m^{-2} s^{-1} for the samples collected from 5 m, 25 m, and 50 m, and decreased to ~ 290 μE m^{-2} s^{-1} for the sample collected from 120 m (Fig. 6). In *KK1902*, the surface daily average PAR during incubations which were higher than 725 μE m^{-2} s^{-1} (S21 was excluded due to the cloudy weather during incubation, Fig. S6), indicating in-situ surface NFR were inhibited by high light intensity over 725 μE m^{-2} s^{-1}. For photosynthetic diazotrophs, high light intensity inhibits nitrogen fixation which may result from photorespiration energy dissipation, then energy or proton restriction may lead to reduced NFR (Long et al., 1994). On the other hand, the optimal light intensity for NFR at 50 m and 120 m was higher than in-situ light intensity at these depths, suggesting that diazotrophs were light-limited there (Fig. 6). The maximum NFR were observed at the depth where optimal light intensity was close to the in-situ light intensity. Our results indicate that light intensity attenuation is responsible for the vertically unimodal pattern of NFR where photoautotrophic cyanobacterial diazotrophs dominated. This vertically unimodal distribution of NFR maybe a basin-scale characteristic rather than a unique feature for CEs as the vertical light attenuation is expected to affect nitrogen fixation in broad oligotrophic ocean regions. Meanwhile, our light manipulation incubations provided evidence of light stimulation on nitrogen fixation rates in the process of upwelling.

In *KK1902*, we found that the vertical highest NFR at the investigated stations was located at about 30 m depth, consistent with previous

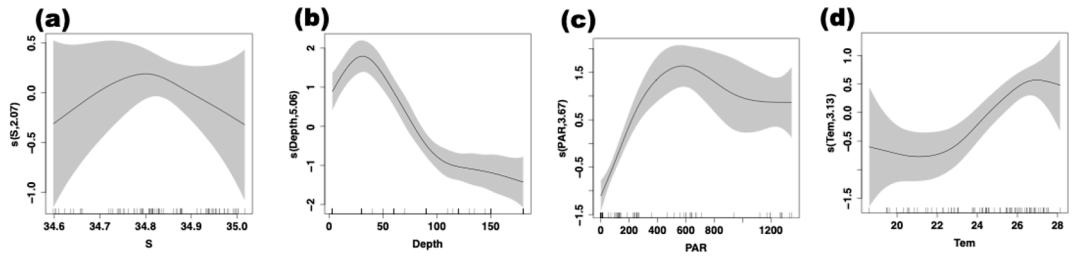

Fig. 7. Non-linear correlations between NFR and environmental parameters. (a), Partial effects of salinity (S) (a), Depth (b), incubation PAR (c), and temperature (Tem) (d) on corresponding NFRs in all layers in 11 stations using the GAM multivariate analysis show here. Grey shadows are corresponded to the 95% confidence intervals.

research (Lu et al., 2019; Shiozaki et al., 2017; Wen et al., 2022), with the corresponding in-situ daily average light intensity of approximately 380 μE m^{-2} s^{-1}, which was calculated by using an average light attenuation coefficient of 0.0415 and a daily average sPAR on deck in *KK1902* (Fig. S6; Table 1). However, the GAM results suggested that the NFR peaks at around 550 μE m^{-2} s^{-1} (light intensity for incubations, calculated by sPAR on deck and light shading coefficient by optical filter) (Fig. 7 c; Fig. S6). Light intensity for incubations was a little higher than in-situ light intensity, which might result in an uncertainty of NFR at this cruise. On the other hand, both light intensity for incubations and in-situ light intensity were less than optimal light intensity in the upper 50 m in the *KK2007*, indicating a true depth with the NFR maximum was above 30 m which we might miss in the *KK1902*. Therefore, a higher spatial resolution sampling strategy was needed in the upper 30 m in the further study to get a more accurate INFR.

Additionally, as temperature was found to limit diazotrophic growth in previous research (Fu et al., 2014), our findings showed low NFR in water with low temperature (Fig. 7 d). Therefore, upwelling of this subsurface water benefits nitrogen fixation by alleviating light and temperature limitation before other nutrients, such as phosphate and iron, become limiting factors for the growth of diazotrophs.

The results provided evidence of the stimulation of nitrogen fixation due to the CEs-induced upwelling, as the entrainment of a water mass with a salinity of 34.8 ± 0.1 from about 150 m into the optimal light zone for diazotrophs (20 % − 50 % of sPAR). However, Excessive intensity of upwelling and light intensity may result in reduced nitrogen fixation rates. Therefore, we proposed a physical optima for nitrogen fixation in cyclonic eddies in the Subtropical Northwestern Pacific based on non-linear responses of nitrogen fixation to the upwelling intensity and light intensity (Fig. 8).

4.3. *UCYN-A was more competitive than UCYN-B in the process of upwelling*

UCYN-A and UCYN-B dominated in the CE2, being consistent with previous observations in the study area at different years and seasons (Fig. 5), suggesting a regional dominance of diazotrophs by the unicellular cyanobacteria in the Subtropical Northwestern Pacific (Chen et al., 2019; Wen et al., 2022). In this study, *nifH* gene copies of UCYN-A were higher than that of UCYN-B in stations (Z2, Z6, and 3Z1) where water with a salinity of 34.8 ± 0.1 reached depth with optimal light for nitrogen fixation, which indicated CEs-induced upwelling may be favored for UCYN-A than UCYN-B (Fig. 5; Fig. S4). UCYN-A dominated in the upwelling area which were reported in recent years (Liu et al., 2023a,b; Cheung et al., 2020; Horii et al.,2023). UCYN-A has been recently identified as ubiquitous in the global ocean spanning from oligotrophic gyres to the eutrophic coastal waters and the low-temperature polar seas, attributed to their good adaptation in high-nutrient and low-temperature environments (Harding et al. 2018; Mills et al., 2020; Tang et al. 2019; Shiozaki et al., 2020). Indeed, the presence of nitrate has been found to favor the growth of UCYN-A, as enriched nitrate stimulates photosynthesis of the host haptophyte alga, which serves as the organic carbon source for the symbiont diazotroph (Thompson et al., 2012; Mills et al., 2020). Nitrate stimulated their host may simultaneously enhance the growth of UCYN-A. Although researches had revealed that nitrate may not inhibit UCYN-B (Dekaezemacker and Bonnet, 2011; Rabouille et al., 2021). The surface temperature of the upwelled water (at 26.7 ± 0.6℃) in this study was lower than the optimal temperature for UCYN-B (at around 30℃) (Fu et al., 2014), indicating temperature may limit UCYN-B in the process of upwelling, which was consistent with our results revealing the abundance peak of UCYN-A at around 25 ℃ and UCYN-B at around 27 ℃ (Fig. S7).

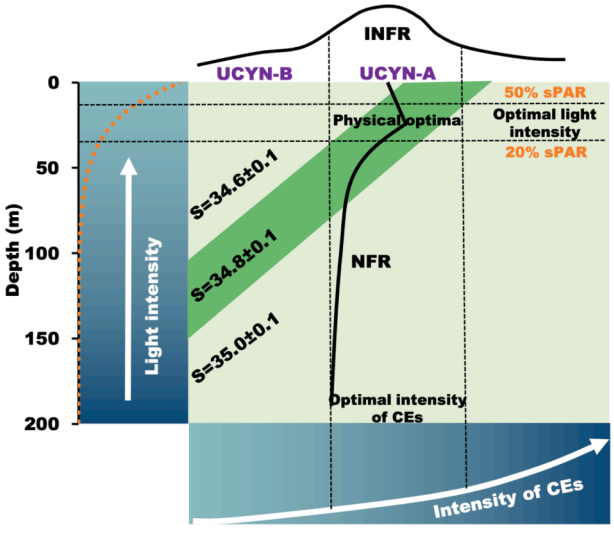

Fig. 8. Conceptual diagram of physical optima for nitrogen fixation involving optimum light intensity and optimum intensity of CEs.

In this study, the diazotrophic community was dominated by the photoautotrophic UCYN-A and UCYN-B (Fig. 5), indicating a dependence of nitrogen fixation on light. Moreover, different taxa display different light affinities, leading to the vertical niche separation along the water column (Breitbarth et al., 2008; Foster et al., 2010; Garcia et al., 2013; Villareal, 1990; Pyle et al., 2020; Villareal, 1990). Lab culture and culture-independent approach showed that the saturated light intensity for UCYN-B (83 ± 13 μE m^{-2} s^{-1}) was higher than that of UCYN-A (44 ± 23 μE m^{-2} s^{-1}) (Garcia et al., 2013; Gradoville et al., 2021), indicating low light adaptation for UCYN-A. Our results are consistent with this finding, as *nifH* gene copies of UCYN-A were higher than UCYN-B in the low-light deeper euphotic zone (Fig. 5). However, the reported optimal light intensities for nitrogen fixation in the field studies were significantly higher than the results from lab culture (Lu et al., 2019). The underlying cause for such discrepancy might be due to low-light acclimation in lab cultures or higher light requirement for diazotrophs in the field to resist the pressure of existence (low nutrients level or grazer, etc.). Our study implied that UCYN-A having more advantages than UCYN-B in upwelling areas due to UCYN-A's physiological property to adapt to low temperatures and high nitrate conditions. Therefore, we suggested that eddy-induced physical perturbation modifies the niches of diazotrophs in the upper euphotic zone.

5. Conclusion

Nitrogen fixation has been widely assumed to be inhibited by the CEs, owing to the supply of cold and nitrogen-enriched water (Dekaezemacker and Bonnet, 2011; Holl and Montoya, 2005; Holl et al., 2007; Luo et al., 2012). However, direct observations of the impact of CEs on nitrogen fixation remain numbered (Liu et al., 2020; Dugenne et al., 2023). Our investigations on NFR and diazotrophic distribution in two CEs in the Subtropical Northwest Pacific revealed that CEs-induced upwelling exerts a unimodal control on marine nitrogen fixation depending on the intensity of upwelling. Combined with the light manipulation incubations, we demonstrated that light acted as a key control for the vertically unimodal distribution of NFR. Our results also revealed that UCYN-A was more competitive than UCYN-B in the upwelling areas.

Together, our results suggested that physical processes play a significant role in controlling the heterogeneity of diazotrophic distribution and activity in the ocean, providing a new understanding of the varied responses of nitrogen fixation to the physical processes in the global ocean. These findings should improve our ability to constrain the biogeographic distribution of nitrogen fixation and to model nitrogen cycling in the global relevant physical process.

Author Contribution Statement

Hui Shen and Shuh-Ji Kao designed this study. Hui Shen, Xianhui S. Wan, Wenbin Zou, Mingming Chen, conducted field sampling and measured the samples. Zhendong Hu, Kuanbo Zhou, Zongpei Jiang provided the physical and hydrological data collection and analysis. Shuh-Ji Kao, Yao Zhang and Minhan Dai provided the research resources. Hui Shen wrote the manuscript with input from Shuh-Ji Kao, Xianhui S. Wan and Senwei Tong. All authors discussed and edited the manuscript.

CRediT authorship contribution statement

Hui Shen: Data curation, Formal analysis, Investigation, Methodology, Writing – original draft, Writing – review & editing. **Xianhui S. Wan:** Data curation, Investigation, Writing – review & editing. **Wenbin Zou:** Investigation, Resources. **Mingming Chen:** Data curation. **Zhendong Hu:** Data curation. **Senwei Tong:** Writing – review & editing. **Kuanbo Zhou:** Investigation. **Zong-Pei Jiang:** Investigation. **Yao Zhang:** Data curation. **Minhan Dai:** Funding acquisition, Writing – review & editing. **Shuh-Ji Kao:** Funding acquisition, Writing – review & editing.

Declaration of competing interest

The authors declare that they have no known competing financial interests or personal relationships that could have appeared to influence the work reported in this paper.

Data availability

Data will be made available on request.

Acknowledgment

The authors greatly appreciate the help of X. Tian and J. Yang during the research cruise to the Northwest Pacific. We also thank S. Wu and M. Du for their technical support. We acknowledge the captain and crew of the R/V *Tan Kah Kee* for the help during the cruises. This work was supported by the National Natural Science Foundation of China (92058204, 41730533, 41890802, 42049582).

Appendix A. Supplementary data

Supplementary data to this article can be found online at https://doi.org/10.1016/j.pocean.2024.103298.

References

Benavides, M., Conradt, L., Bonnet, S., Berman-Frank, I., Barrillon, S., Petrenko, A., Doglioli, A., 2021. Fine-scale sampling unveils diazotroph patchiness in the South Pacific Ocean. ISME Communications 1 (1), 3.

Benavides, M., Robidart, J., 2020. Bridging the spatiotemporal gap in diazotroph activity and diversity with high-resolution measurements. Front. Mar. Sci. 7, 568876.

Bonnet, S., Benavides, M., Le Moigne, F.A., Camps, M., Torremocha, A., Grosso, O., Cornejo-Castillo, F.M., 2023a. Diazotrophs are overlooked contributors to carbon and nitrogen export to the deep ocean. ISME J. 17 (1), 47–58.

Bonnet, S., Guieu, C., Taillandier, V., Boulart, C., Bouruet-Aubertot, P., Gazeau, F., Tilliette, C., 2023b. Natural iron fertilization by shallow hydrothermal sources fuels diazotroph blooms in the ocean. Science 380 (6647), 812–817.

Böttjer, D., Dore, J.E., Karl, D.M., Letelier, R.M., Mahaffey, C., Wilson, S.T., Church, M.J., 2017. Temporal variability of nitrogen fixation and particulate nitrogen export at Station ALOHA. Limnol. Oceanogr. 62 (1), 200–216.

Boyd, P.W., Ellwood, M.J., 2010. The biogeochemical cycle of iron in the ocean. Nat. Geosci. 3 (10), 675–682.

Braman, R.S., Hendrix, S.A., 1989. Nanogram nitrite and nitrate determination in environmental and biological materials by vanadium (III) reduction with chemiluminescence detection. Anal. Chem. 61 (24), 2715–2718.

Breitbarth, E., Wohlers, J., Kläs, J., LaRoche, J., Peeken, I., 2008. Nitrogen fixation and growth rates of *Trichodesmium* IMS-101 as a function of light intensity. Mar. Ecol. Prog. Ser. 359, 25–36.

Casciotti, K.L., Sigman, D.M., Hastings, M.G., Böhlke, J.K., Hilkert, A., 2002. Measurement of the oxygen isotopic composition of nitrate in seawater and freshwater using the denitrifier method. Anal. Chem. 74 (19), 4905–4912.

Chang, B.X., Jayakumar, A., Widner, B., Bernhardt, P., Mordy, C.W., Mulholland, M.R., Ward, B.B., 2019. Low rates of dinitrogen fixation in the eastern tropical South Pacific. Limnol. Oceanogr. 64 (5), 1913–1923.

Chen, M., Lu, Y., Jiao, N., Tian, J., Kao, S.J., Zhang, Y., 2019. Biogeographic drivers of diazotrophs in the western Pacific Ocean. Limnol. Oceanogr. 64 (3), 1403–1421.

Cheung, S., Nitanai, R., Tsurumoto, C., Endo, H., Nakaoka, S.I., Cheah, W., Suzuki, K., 2020. Physical forcing controls the basin-scale occurrence of nitrogen-fixing organisms in the North Pacific Ocean. Global Biogeochem. Cycles 34 (9) e2019GB006452.

Church, M.J., Short, C.M., Jenkins, B.D., Karl, D.M., Zehr, J.P., 2005. Temporal patterns of nitrogenase gene (*nifH*) expression in the oligotrophic North Pacific Ocean. Appl. Environ. Microbiol. 71 (9), 5362–5370.

Church, M.J., Mahaffey, C., Letelier, R.M., Lukas, R., Zehr, J.P., Karl, D.M., 2009. Physical forcing of nitrogen fixation and diazotroph community structure in the North Pacific subtropical gyre. Global Biogeochem. Cycles 23 (2).

Davis, C.S., McGillicuddy Jr, D.J., 2006. Transatlantic abundance of the N_2-fixing colonial cyanobacterium *Trichodesmium*. Science 312 (5779), 1517–1520.

Dekaezemacker, J., Bonnet, S., 2011. Sensitivity of N_2 fixation to combined nitrogen forms (NO_3^- and NH_4^+) in two strains of the marine diazotroph *Crocosphaera watsonii* (Cyanobacteria). Mar. Ecol. Prog. Ser. 438, 33–46.

Deutsch, C., Sarmiento, J.L., Sigman, D.M., Gruber, N., Dunne, J.P., 2007. Spatial coupling of nitrogen inputs and losses in the ocean. Nature 445 (7124), 163–167.

Dugdale, R.C., 1961. Nitrogen fixation in the Sargasso Sea. Deep-Sea Res. 7, 298–300.

Dugdale, R.C., Goering, J.J., Ryther, J.H., 1964. High nitrogen fixation rates in the Sargasso Sea and the Arabian sea. Limnol. Oceanogr. 9 (4), 507–510.

Dugenne, M., Gradoville, M.R., Church, M.J., Barone, B., Wilson, S.T., Sheyn, U., Zehr, J. P., 2023. Nitrogen fixation in mesoscale eddies of the North Pacific Subtropical Gyre: patterns and mechanisms. Global Biogeochem. Cycles 37 e2022GB007386.

Falkowski, P.G., 1997. Evolution of the nitrogen cycle and its influence on the biological sequestration of CO_2 in the ocean. Nature 387 (6630), 272–275.

Falkowski, P.G., Raven, J.A., 2013. Aquatic photosynthesis. Princeton University Press.

Falkowski, P.G., Ziemann, D., Kolber, Z., Bienfang, P.K., 1991. Role of eddy pumping in enhancing primary production in the ocean. Nature 352 (6330), 55–58.

Farnelid, H., Turk-Kubo, K., Ploug, H., Ossolinski, J.E., Collins, J.R., Van Mooy, B.A., Zehr, J.P., 2019. Diverse diazotrophs are present on sinking particles in the North Pacific Subtropical Gyre. ISME J. 13 (1), 170–182.

Fong, A.A., Karl, D.M., Lukas, R., Letelier, R.M., Zehr, J.P., Church, M.J., 2008. Nitrogen fixation in an anticyclonic eddy in the oligotrophic North Pacific Ocean. ISME J. 2 (6), 663–676.

Foster, R.A., Subramaniam, A., Mahaffey, C., Carpenter, E.J., Capone, D.G., Zehr, J.P., 2007. Influence of the Amazon River plume on distributions of free-living and symbiotic cyanobacteria in the western tropical North Atlantic Ocean. Limnol. Oceanogr. 52 (2), 517–532.

Foster, R.A., Goebel, N.L., Zehr, J.P., 2010. Isolation of *Calothrix Rhizosoleniae* (cyanobacteria) strain SC01 from *Chaetoceros* (bacillariophyta) spp. diatoms of the Subtropical North Pacific Ocean. J. Phycol. 46 (5), 1028–1037.

Fu, F.X., Yu, E., Garcia, N.S., Gale, J., Luo, Y., Webb, E.A., Hutchins, D.A., 2014. Differing responses of marine N_2 fixers to warming and consequences for future diazotroph community structure. Aquat. Microb. Ecol. 72 (1), 33–46.

Garcia, N.S., Fu, F.X., Hutchins, D.A., 2013. Colimitation of the unicellular photosynthetic diazotroph *Crocosphaera watsonii* by phosphorus, light, and carbon dioxide. Limnol. Oceanogr. 58 (4), 1501–1512.

Gradoville, M. R., Cabello, A. M., Wilson, S. T., Turk-Kubo, K. A., Karl, D. M., & Zehr, J. P. (2021). Light and depth dependency of nitrogen fixation by the non-photosynthetic, symbiotic cyanobacterium UCYN-A. *Environmental microbiology*, *23* (8), 4518-4531.

Gruber, N., Lachkar, Z., Frenzel, H., Marchesiello, P., Münnich, M., McWilliams, J.C., Plattner, G.K., 2011. Eddy-induced reduction of biological production in eastern boundary upwelling systems. Nat. Geosci. 4 (11), 787–792.

Gruber, N., Sarmiento, J.L., 1997. Global patterns of marine nitrogen fixation and denitrification. Global Biogeochem. Cycles 11 (2), 235–266.

Guo, M., Xiu, P., Xing, X., 2022. Oceanic fronts structure phytoplankton distributions in the central South Indian Ocean. J. Geophys. Res. Oceans 127 (1) e2021JC017594.

Guo, M., Xing, X., Xiu, P., Dall'Olmo, G., Chen, W., Chai, F., 2024. Efficient biological carbon export to the mesopelagic ocean induced by submesoscale fronts. Nat. Commun. 15 (1), 1–10.

Harding, K., Turk-Kubo, K.A., Sipler, R.E., Mills, M.M., Bronk, D.A., Zehr, J.P., 2018. Symbiotic unicellular cyanobacteria fix nitrogen in the Arctic Ocean. Proc. Natl. Acad. Sci. 115 (52), 13371–13375.

Holl, C.M., Montoya, J.P., 2005. Interactions between nitrate uptake and nitrogen fixation in continuous cultures of the marine diazotroph *Trichodesmium* (cyanobacteria). J. Phycol. 41 (6), 1178–1183.

Holl, C.M., Waite, A.M., Pesant, S., Thompson, P.A., Montoya, J.P., 2007. Unicellular diazotrophy as a source of nitrogen to Leeuwin Current coastal eddies. Deep-Sea Res. II Top. Stud. Oceanogr. 54 (8–10), 1045–1054.

Horii, S., Takahashi, K., Shiozaki, T., Takeda, S., Sato, M., Yamaguchi, T., Furuya, K., 2023. East-West Variabilities of N_2 Fixation Activity in the Subtropical North Pacific Ocean in Summer: Potential Field Evidence of the Phosphorus and Iron Co-Limitation in the Western Area. J. Geophys. Res. Oceans 128 (6) e2022JC019249.

Kara, A.B., Rochford, P.A., Hurlburt, H.E., 2000. An optimal definition for ocean mixed layer depth. J. Geophys. Res. Oceans 105 (C7), 16803–16821.

Karl, D. M., Church, M. J., Dore, J. E., Letelier, R. M., & Mahaffey, C. (2012). Predictable and efficient carbon sequestration in the North Pacific Ocean supported by symbiotic nitrogen fixation. *Proceedings of the National Academy of Sciences*, *109*(6), 1842-1849.
Karl, D., Letelier, R., Tupas, L., Dore, J., Christian, J., Hebel, D., 1997. The role of nitrogen fixation in biogeochemical cycling in the subtropical North Pacific Ocean. Nature 388 (6642), 533–538.
Karl, D.M., Letelier, R.M., 2008. Nitrogen fixation-enhanced carbon sequestration in low nitrate, low chlorophyll seascapes. Mar. Ecol. Prog. Ser. 364, 257–268.
Kitajima, S., Furuya, K., Hashihama, F., Takeda, S., Kanda, J., 2009. Latitudinal distribution of diazotrophs and their nitrogen fixation in the tropical and subtropical western North Pacific. Limnol. Oceanogr. 54 (2), 537–547.
Knapp, A.N., Sigman, D.M., Lipschultz, F., 2005. N isotopic composition of dissolved organic nitrogen and nitrate at the Bermuda Atlantic Time-series Study site. Global Biogeochem. Cycles 19 (1).
Liu, H., Browning, T.J., Laws, E.A., Huang, Y., Wang, L., Shang, Y., Dai, M., 2024. Stimulation of small phytoplankton drives enhanced sinking particle formation in a subtropical ocean eddy. Limnology and. Oceanography.
Liu, L., Chen, M., Wan, X.S., Du, C., Liu, Z., Hu, Z., Zhang, Y., 2023a. Reduced nitrite accumulation at the primary nitrite maximum in the cyclonic eddies in the western North Pacific subtropical gyre. Sci. Adv. 9 (33), eade2078.
Liu, J., Zhou, L., Li, J., Lin, Y., Ke, Z., Zhao, C., Tan, Y., 2020. Effect of mesoscale eddies on diazotroph community structure and nitrogen fixation rates in the South China Sea. Reg. Stud. Mar. Sci. 35, 101106.
Liu, J., Zhang, H., Ding, X., Zhou, L., Ke, Z., Li, J., Tan, Y., 2023b. Nitrogen fixation under the interaction of Kuroshio and upwelling in the northeastern South China Sea. Deep-Sea Res. I Oceanogr. Res. Pap. 200, 104147.
Long, S.P., Humphries, S., Falkowski, P.G., 1994. Photoinhibition of photosynthesis in nature. Annu. Rev. Plant Biol. 45 (1), 633–662.
Lu, Y., Wen, Z., Shi, D., Chen, M., Zhang, Y., Bonnet, S., Kao, S.J., 2018. Effect of light on N_2 fixation and net nitrogen release of *Trichodesmium* in a field study. Biogeosciences 15 (1), 1–12.
Lu, Y., Wen, Z., Shi, D., Lin, W., Bonnet, S., Dai, M., Kao, S.J., 2019. Biogeography of N_2 fixation influenced by the western boundary current intrusion in the South China Sea. J. Geophys. Res. Oceans 124 (10), 6983–6996.
Luo, Y.W., Doney, S.C., Anderson, L.A., Benavides, M., Berman-Frank, I., Bode, A., Zehr, J.P., 2012. Database of diazotrophs in global ocean: abundance, biomass and nitrogen fixation rates. Earth Syst. Sci. Data 4 (1), 47–73.
Massana, R., Murray, A.E., Preston, C.M., DeLong, E.F., 1997. Vertical distribution and phylogenetic characterization of marine planktonic Archaea in the Santa Barbara Channel. Appl. Environ. Microbiol. 63 (1), 50–56.
McGillicuddy Jr, D.J., 2016. Mechanisms of physical-biological-biogeochemical interaction at the oceanic mesoscale. Ann. Rev. Mar. Sci. 8, 125–159.
Mills, M.M., Turk-Kubo, K.A., van Dijken, G.L., Henke, B.A., Harding, K., Wilson, S.T., Zehr, J.P., 2020. Unusual marine cyanobacteria/haptophyte symbiosis relies on N2 fixation even in N-rich environments. ISME J. 14 (10), 2395–2406.
Mohr, W., Grosskopf, T., Wallace, D.W., LaRoche, J., 2010. Methodological underestimation of oceanic nitrogen fixation rates. PLoS One 5 (9), e12583.
Moisander, P.H., Beinart, R.A., Voss, M., Zehr, J.P., 2008. Diversity and abundance of diazotrophic microorganisms in the South China Sea during intermonsoon. ISME J. 2 (9), 954–967.
Montoya, J.P., Voss, M., Kahler, P., Capone, D.G., 1996. A simple, high-precision, high-sensitivity tracer assay for N_2 fixation. Appl. Environ. Microbiol. 62 (3), 986–993.
Moore, C.M., Mills, M.M., Arrigo, K.R., Berman-Frank, I., Bopp, L., Boyd, P.W., Ulloa, O., 2013. Processes and patterns of oceanic nutrient limitation. Nat. Geosci. 6 (9), 701–710.
Oschlies, A., Garçon, V., 1998. Eddy-induced enhancement of primary production in a model of the North Atlantic Ocean. Nature 394 (6690), 266–269.
Pyle, A.E., Johnson, A.M., Villareal, T.A., 2020. Isolation, growth, and nitrogen fixation rates of the *Hemiaulus-Richelia* (diatom-cyanobacterium) symbiosis in culture. PeerJ 8, e10115.
Qiu, B., 1999. Seasonal eddy field modulation of the North Pacific Subtropical Countercurrent: TOPEX/Poseidon observations and theory. J. Phys. Oceanogr. 29 (10), 2471–2486.
Qiu, B., Lukas, R., 1996. Seasonal and interannual variability of the North Equatorial Current, the Mindanao Current, and the Kuroshio along the Pacific western boundary. J. Geophys. Res. Oceans 101 (C5), 12315–12330.
Rabouille, S., Randall, B., Talec, A., Raimbault, P., Blasco, T., Latifi, A., Oschlies, A., 2021. Independence of a Marine Unicellular Diazotroph to the Presence of NO_3^-. Microorganisms 9 (10), 2073.
Rohr, T., Harrison, C., Long, M.C., Gaube, P., Doney, S.C., 2020. Eddy-modified iron, light, and phytoplankton cell division rates in the simulated Southern Ocean. Global Biogeochem. Cycles 34 (6) e2019GB006380.
Shiozaki, T., Bombar, D., Riemann, L., Hashihama, F., Takeda, S., Yamaguchi, T., Furuya, K., 2017. Basin scale variability of active diazotrophs and nitrogen fixation in the North Pacific, from the tropics to the subarctic Bering Sea. Global Biogeochem. Cycles 31 (6), 996–1009.
Shiozaki, T., Fujiwara, A., Inomura, K., Hirose, Y., Hashihama, F., Harada, N., 2020. Biological nitrogen fixation detected under Antarctic Sea ice. Nat. Geosci. 13 (11), 729–732.
Sigman, D.M., Casciotti, K.L., Andreani, M., Barford, C., Galanter, M.B.J.K., Böhlke, J.K., 2001. A bacterial method for the nitrogen isotopic analysis of nitrate in seawater and freshwater. Anal. Chem. 73 (17), 4145–4153.
Sohm, J.A., Webb, E.A., Capone, D.G., 2011. Emerging patterns of marine nitrogen fixation. Nat. Rev. Microbiol. 9 (7), 499–508.
Subramaniam, A., Mahaffey, C., Johns, W., Mahowald, N., 2013. Equatorial upwelling enhances nitrogen fixation in the Atlantic Ocean. Geophys. Res. Lett. 40 (9), 1766–1771.
Tang, W., Wang, S., Fonseca-Batista, D., Dehairs, F., Gifford, S., Gonzalez, A.G., Cassar, N., 2019. Revisiting the distribution of oceanic N_2 fixation and estimating diazotrophic contribution to marine production. Nat. Commun. 10 (1), 831.
Thompson, A., Carter, B.J., Turk-Kubo, K., Malfatti, F., Azam, F., Zehr, J.P., 2014. Genetic diversity of the unicellular nitrogen-fixing cyanobacteria UCYN-A and its prymnesiophyte host. Environ. Microbiol. 16 (10), 3238–3249.
Thompson, A.W., Foster, R.A., Krupke, A., Carter, B.J., Musat, N., Vaulot, D., Zehr, J.P., 2012. Unicellular cyanobacterium symbiotic with a single-celled eukaryotic alga. Science 337 (6101), 1546–1550.
Toole, J.M., Millard, R.C., Wang, Z., Pu, S., 1990. Observations of the Pacific North Equatorial Current bifurcation at the Philippine coast. J. Phys. Oceanogr. 20 (2), 307–318.
Villareal, T.A., 1990. Laboratory culture and preliminary characterization of the nitrogen-fixing *Rhizosolenia-Richelia* symbiosis. Mar. Ecol. 11 (2), 117–132.
Wan, X.S., Sheng, H.X., Dai, M., Zhang, Y., Shi, D., Trull, T.W., Kao, S.J., 2018. Ambient nitrate switches the ammonium consumption pathway in the euphotic ocean. Nat. Commun. 9 (1), 915.
Wang, H., Luo, Y.W., 2022. Top-down control on major groups of global marine diazotrophs. Acta Oceanol. Sin. 41 (8), 111–119.
Wang, W.L., Moore, J.K., Martiny, A.C., Primeau, F.W., 2019. Convergent estimates of marine nitrogen fixation. Nature 566 (7743), 205–211.
Ward, B.A., Dutkiewicz, S., Moore, C.M., Follows, M.J., 2013. Iron, phosphorus, and nitrogen supply ratios define the biogeography of nitrogen fixation. Limnol. Oceanogr. 58 (6), 2059–2075.
Webb, W.L., Newton, M., Starr, D., 1974. Carbon dioxide exchange of Alnus rubra: a mathematical model. Oecologia 17, 281–291.
Wen, Z., Browning, T.J., Cai, Y., Dai, R., Zhang, R., Du, C., Shi, D., 2022. Nutrient regulation of biological nitrogen fixation across the tropical western North Pacific. Sci. Adv. 8 (5), eabl7564.
White, A.E., Granger, J., Selden, C., Gradoville, M.R., Potts, L., Bourbonnais, A., Chang, B.X., 2020. A critical review of the $^{15}N_2$ tracer method to measure diazotrophic production in pelagic ecosystems. Limnol. Oceanogr. Methods 18 (4), 129–147.
Wilson, S.T., Böttjer, D., Church, M.J., Karl, D.M., 2012. Comparative assessment of nitrogen fixation methodologies, conducted in the oligotrophic North Pacific Ocean. Appl. Environ. Microbiol. 78 (18), 6516–6523.
Wilson, S.T., Aylward, F.O., Ribalet, F., Barone, B., Casey, J.R., Connell, P.E., DeLong, E. F., 2017. Coordinated regulation of growth, activity and transcription in natural populations of the unicellular nitrogen-fixing cyanobacterium *Crocosphaera*. Nat. Microbiol. 2 (9), 1–9.
Xu, M.N., Li, X., Shi, D., Zhang, Y., Dai, M., Huang, T., Kao, S.J., 2019. Coupled effect of substrate and light on assimilation and oxidation of regenerated nitrogen in the euphotic ocean. Limnol. Oceanogr. 64 (3), 1270–1283.
Yang, G., Wang, F., Li, Y., Lin, P., 2013. Mesoscale eddies in the northwestern subtropical Pacific Ocean: Statistical characteristics and three-dimensional structures. J. Geophys. Res. Oceans 118 (4), 1906–1925.
Yi, X., Fu, F.X., Hutchins, D.A., Gao, K., 2020. Light availability modulates the effects of warming in a marine N_2 fixer. Biogeosciences 17 (4), 1169–1180.
Zehr, J.P., Capone, D.G., 2020. Changing perspectives in marine nitrogen fixation. Science 368 (6492), eaay9514.